Simulation for Low Temperature Coefficient Design of Piezoresistive and Hall Sensors

K. Matsuda* and Y. Kanda**

*Naruto University of Education, 748 Nakashima, Takashima, Naruto-cho, Naruto 772-8502, Japan, matsudak@naruto-u.ac.jp
**Facalty of Engineering and Bio-nano Electronics Research Center, Toyo University, 2100 Kujirai, Kawagoe Saitama 350-8585, Japan, yozo@eng.toyo.ac.jp

ABSTRACT

Simulation for the temperature coefficient of piezoresistive and Hall sensors is presented. Carrier and ionized impurity concentrations in the *n*-type silicon gage are calculated from the charge balance equation by applying Newton iteration scheme. The impurity band and the tail of band edge are taken into account as the density-of-state functions. The electron mobility is calculated by appropriately combing lattice, ionized impurity and neutral impurity scattering. The effect of electron-electron scattering is incorporated in the relaxation time of each scattering. The dependencies of temperature and impurity concentrations for electron mobility are simultaneously obtained. The temperature coefficients of the piezoresistance and Hall coefficients are computed as the functions of dopant concentrations.

Keywords: mobility, sensor, TC, piezoresistance, Hall.

1 INTRODUCTION

Temperature coefficient (TC) of sensors affects the accuracy of their operations. Although it is empirically known that the TC of piezoresitive sensors can be reduced by using heavily doped silicon resistance layers, the knowledge on the TC of piezoresitance (TCPR) as a function of the dopant concentration and the type of dopant must be prerequisite to design high precision sensors.

Previously we simulated the influence of heavy doping on the TC of the piezoresistive sensor [1]. In this simulation the impurity band and the tail of the band edge formed by the interaction of the impurity atoms were taken into account in the density-of-state (DOS) functions, and solved the charge balance equation to find the Fermi energy by applying Newton iteration scheme. The TCPR was simulated by Fermi-Dirac approximation using this Fermi energy. However, this simulation was needed to the effect of impurity on the mobility for wide concentration range, which remained as a future problem.

In the present study we propose a model by using the generalized PR factor which includes a strict mobility simulation. For the mobility model, the contribution from scattering by lattice phonons, ionized impurities and neutral impurities are properly combined.

As the results, the TCPR simulation is discussed on its feasibility by comparing available experimental data. This model is also applied to Hall mobility, and the simulation for TC of Hall sensors is made.

2 SENSOR SIMULATION SCHEME

The simulation is composed of three parts. The first part solves the charge balance equation and obtains Fermi energy. Then electron mobility is computed in the next part. Final part is the simulation for the piezoresistive and Hall sensors, where the PR and the Hall factors are calculated. Simulations for TC are made by varying temperature input of the first part and by taking the derivative due to the differential calculus. Each part will be briefly described in the following sub-section.

2.1 Carrier Concentrations

The carrier concentrations and ionized impurities concentrations are obtained by solving the charge balance equation defined by the impurity concentrations and the temperature.

$$p(F)+N_D^+(F)=n(F)+N_A^-(F) \qquad (1)$$

where $p(F)$, $n(F)$, $N_A^-(F)$ and $N_D^+(F)$ are the total electron and hole, the ionized donor and ionized acceptor concentrations respectively. Newton-iteration scheme is applied to solve this equation for Fermi energy F. The integrals appeared in the calculations of carrier concentration are same as the Fermi integral except that the DOS functions are used instead of the square-root DOS. The computation scheme in this part is same as our previous paper [1]. However following problems are revised.

1. The generalized screening length _ is adopted in stead of Debye length [2]

$$\lambda^{-2}=\frac{q^2}{\varepsilon}\left(\left|\frac{fn}{fF}\right|+\left|\frac{fp}{fF}\right|+\frac{N_D^+ + N_A^-}{E_{ion}}\right) \qquad (2)$$

where E_{ion} is the effective energy for screening which is about 7000 K. The screening length is solved consistently with Eq. 1.

2. In the calculation of ionized acceptor, the ground state degeneracy and the contribution of the excited state between the ground state and the split-orbit sprit bands are taken into account.
3. The dependencies of ionization energies on dopant concentrations are implemented.

2.2 Mobility

Phonon scattering mechanisms of electrons are intravalley scattering and intervalley scattering. The transverse phonon scattering rate is generally can be written as,

$$\frac{1}{\tau_{L\perp}}=\frac{1}{\tau_0 T^{-3/2}}(x^{1/2}+\sum_i\{w_i(\theta_i/T)[n_i(x+\theta_i/T)^{1/2} +(n_i+1)(x-\theta_i/T)^{1/2}]\}) \quad (3)$$

where $x=E/kT$ and E represents the electron energy, θ_I is the temperature of the ith intervalley phonon, $n_i=[\exp(\theta_i/T)-1]^{-1}$ is the phonon distribution function, and w_I is the relative coupling strength of the electrons to the ith intervalley mode compared to the transverse acoustic mode. The parameters used in this calculation are listed in Table 1. The phonon scattering rate in the longitudinal direction is

$$\frac{1}{\tau_{L//}}=\frac{1}{\tau_{L\perp}}+\frac{x^{1/2}}{2\tau_0 T^{-3/2}} \quad (4)$$

τ_0 (10^{-9}sec^{-9})	W_1	W_2	W_3	W_4
3.63	0.0002	1.84	0.080	0.0004

Table 1. Parameters for phonon scattering time. (Coupling constants for intervalley scattering; θ_1=540 K, θ_2=670 K, θ_3=190 K, θ_4=307 K [3].)

Ionized-impurity scattering has been calculated by Brooks and Herring [4]. The scattering rate is given by,

$$\frac{1}{\tau_I}=\frac{q^4 N_I}{16\pi\varepsilon^2(2m^*)^{1/2}(kT)^{3/2}x^{3/2}}\left[\ln(b+1)-\frac{b}{b+1}\right] \quad (5)$$

where

$$b=\frac{2\varepsilon m^*(kT)^2 x}{\pi\hbar^2 q^2 n'},$$

$$n'=n+(n+N_A)[1-(n+N_A)/N_D],.$$

$N_I=N_D^+ + N_A^-$ is the total concentration of ionized impurities, m^* is the conductivity effective mass of electron and ε is the permittivity of silicon. The anisotropic ionized-impurity scattering in a prolate ellipsoidal energy surface is calculated by replacing m^* with longitudinal effective mass $m_{//}$ or transverse effective mass $m_\perp$ in Eq. 5.

Neutral-impurity scattering has been calculated by Erginsoy [5]. The formula can be written as,

$$\frac{1}{\tau_N}=\frac{\varepsilon\hbar^2}{m_d q^2}\left(\frac{20\hbar}{m^*}\right)N_N \quad (6)$$

where $N_N=N_D-N_D^+$ is the concentration of neutral donors, m_d is the density-of-state effective mass. In the calculation of the anisotropic neutral scattering, m^* is also replaced with $m_{//}$ or $m_\perp$.

The expressions of relaxation time described above neglect the effect of electron-electron scattering. The magnitude of the electron-electron scattering is a function of the dependence of the relaxation time on electron energy. Hence the relaxation time for neutral impurity scattering is not affected by the electron-electron scattering. The ratio of relaxation times with and without electron-electron scattering effect has been estimated as 0.88 for phonon scattering, while 0.63 for ionized impurity scattering [6][7].

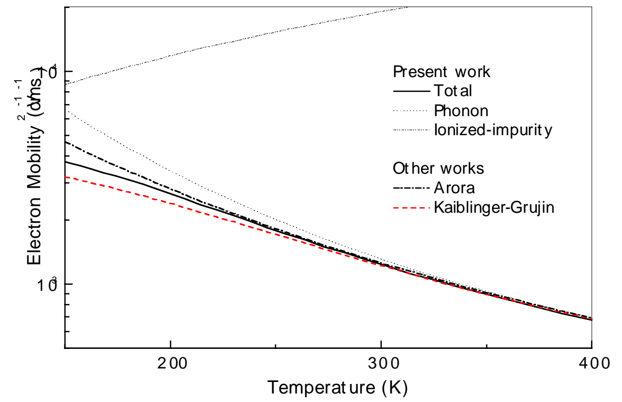

Figure1. Temperature dependence of electron mobiltiy. The donor concentration is 10^{16}cm^{-3}.

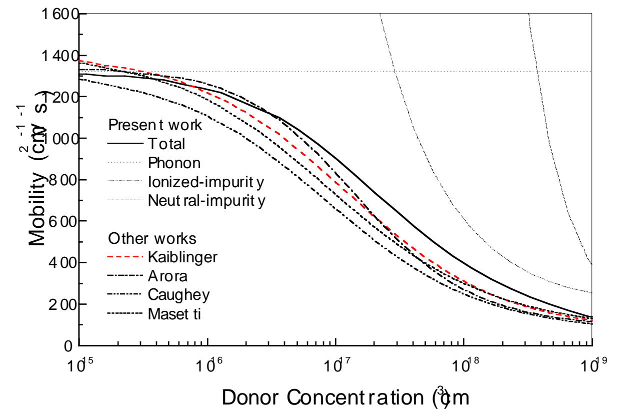

Figure 2. Donor concentration dependence of electron mobility. The temperature is 300 K.

The total relaxation time can be calculated by computing the relaxation time of each scattering process and adding the reciprocal relaxation time for each process, according to Mathieson's rule. As a consequence, the mobility is computed by

$$\mu=\frac{q}{3}\left(\langle\tau_{//}\rangle/m_{//}^{*}+2\langle\tau_{\perp}\rangle/m_{\perp}^{*}\right) \tag{7}$$

where $\langle\tau\rangle$ is the average relaxation time which represents the average over the electron distribution.

2.3 Piezoresistive Sensors

The PR effect of silicon is widely used in pressure sensors, accelerometers and flow sensors. The sensitivity of these sensors is the PR coefficient π, which is defined in terms of the relative resistivity change with stress,

$$\frac{\Delta\rho}{\rho_0}=-\frac{\Delta\sigma}{\sigma_0}=\pi P \tag{8}$$

where _, _ and P are the resistivity, the conductivity and the stress, respectively. According from the many-valley model, the uniaxial stress changes the six band edge energies in a different manner, which induces the electron transfer between the valleys and causes the anisotropic conductivity [8]. In this simulation, we include the stress-induced effect of electron mobility as well as the effect of concentration. In general, the PR coefficient can be expressed by its low-doped room-temperature value. The dependence of the PR coefficients on impurity concentration at a given temperature can be obtained by multiplying the PR factor $P(N_D, N_A, T)$ by the PR coefficient at room temperature [9].

$$P(N_D,N_A,T)=\frac{300}{T}\left[\frac{1}{n}\frac{fn}{fN_D}+\frac{1}{\mu}\frac{f\mu}{fN_D}\right]\left[\frac{f\eta}{fN_D}\right]^{-1} \tag{9}$$

where _ is the reduced Fermi energy. It is worth noticing that the physical values used here, such as n, _, and _, are simply the functions of the impurity concentrations and the temperature.

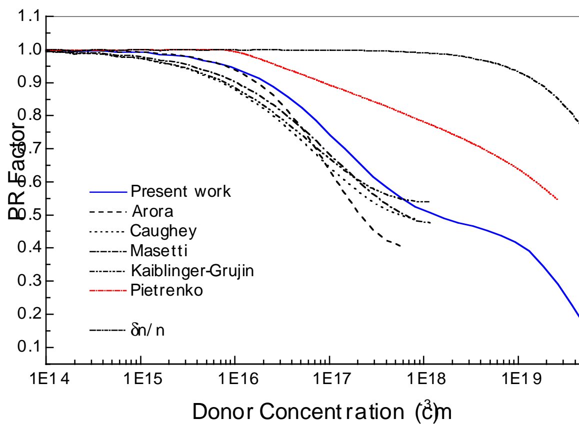

Figure 3. Donor concentration dependence of Piezoresitance Factor. _n/n indicates the electron concentration effect [1]. The short-dashed line is reproduced from the formula of Pietrenko [14.]

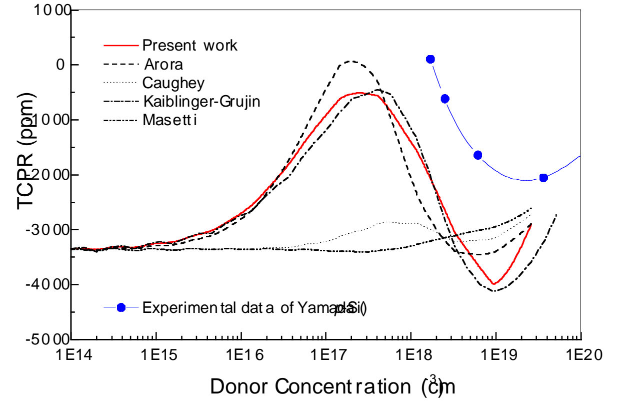

Figure 4. Donor concentration dependence of temperature coefficient of piezoresistance coefficient. The calculations by Caughey and Masetti appear monotonous because the temperature is not explicitly included in their formulas.

2.4 Hall Sensors

The Hall sensors exploit the Lorentz force on moving electrons in silicon, which are used to detect magnetic field, position and displacement of object. The sensitivity of these sensors is the Hall coefficient R_H. The Hall coefficient is defined with the Hall voltage V_H and the magnetic field B as,

$$V_H=R_H IB\sin\alpha/d \tag{10}$$

where _ is the angle between the magnetic field vector and the Hall plate, and d is the thickness of the Hall plate. The Hall coefficient is expressed as,

$$R_H=r_H\frac{1}{nq} \tag{11}$$

where r_H represents the Hall factor. The Hall factor in anisotropic scattering has been described by Herring and Vogt [8]. The expression of r_H is given by,

$$r_H=\frac{3\left\langle\tau_{\perp}^{2}\right\rangle/m_{\perp}^{*2}+2\langle\tau_{\perp}\tau_{//}\rangle/m_{//}^{*}m_{\perp}^{*}}{\left[\langle\tau_{//}\rangle/m_{//}^{*}+2\langle\tau_{\perp}\rangle/m_{\perp}^{*}\right]^{2}} \tag{12}$$

3 RESULTS AND DISUSSIONS

Firstly we discuss about the electron mobility simulation. We have computed the electron mobility using the theoretical expressions. Their inputs are N_D^+, N_A^-, and n, which are obtained by solving the charge valance equation. Some results of the mobility computation are shown in Fig. 1 and Fig. 2. As shown in these figures, the present calculations of the electron mobility reproduce other works fairly well for wide ranges of temperature and impurity concentrations [10][11][12][13]. A slight discrepancy at low temperatures

should be attributed to the combined effect of the ionized-impurity and the phonon scattering. However, it is tolerable here since the sensors usually operate at around room temperature.

In the calculation of the PR effects by Eq. 9, the contribution of the mobility effect is mainly caused from differentiating the stepwise function of the mobility vs. impurity concentration. As shown in Fig. 3, the calculated magnitude of the mobility effect becomes about 25% at the donor concentration 2_10^{17}cm^{-3}. It is known that the TCPR is inversely proportional to $-T$ in lower impurity concentrations and is about 3300 ppm at room temperature. Also, we empirically know that the TCPR can be reduced by heavily doping. As shown in Fig. 4, the simulation results of TCPR have a dull peak around the impurity concentration about 3_10^{17}cm^{-3}, where the TCPR has the minimum value and almost vanishes. This result is consistent with the tendency of the experimental results for *p*-Si by Yamada et al. [15]. However, a room to discuss with experimental data for *n*-Si is left.

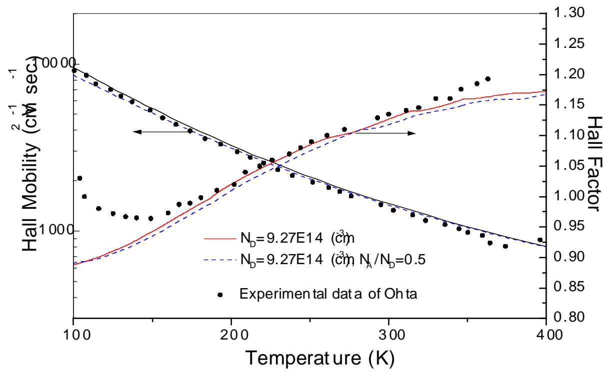

Figure 5. Temperature dependencies of Hall mobility and Hall factor.

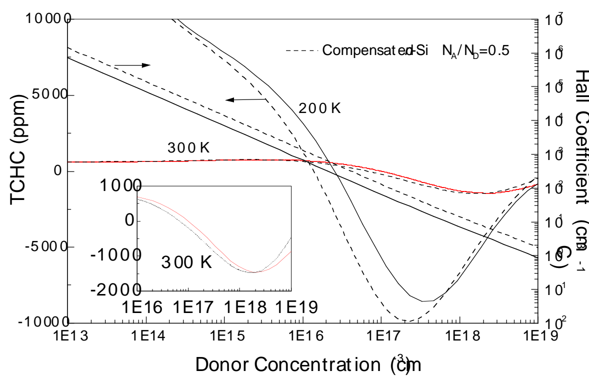

Figure 6. Donor concentration dependencies of temperature coefficient of Hall coefficient and Hall coefficient

There have been a number of papers on the experiments of the Hall coefficient of *n*-Si [15]. The Hall mobility by our computation can reproduce the experimental data very well, as shown in Fig. 5. Some of the computation results of the temperature coefficient of Hall factor are shown in Fig. 6. As shown in this figure the TC of Hall coefficient (TCHC) at room temperature is about 600 ppm for lower donor concentrations. However, it rapidly decreases with increase donor concentration in the region greater than 2_10^{15} cm^{-3} and vanishes at about 9_10^{16} cm^{-3}. While the TCHC at 200 K becomes about 1 % in lower donor concentration regions, and whose vanishing point shifts to lower concentration. The compensation by acceptor makes the Hall coefficient of *n*-Si increase, while which makes the TCHC decrease and shifts its vanishing point to lower concentration. The temperature dependence of the Hall coefficient is not observed

The simulation model presented here is useful in the design to predict lower TC of sensitivity in the piezo-resistive and Hall sensors.

Authors would like to thank Professor D. Vasileska of Arizona State University for her helpful discussions. This work was partially supported by the Special Research Fund of Toyo University.

REFERENCES

[1] K. Matsuda and Y. Kanda, Proc. Modeling and Simulation of Microsystems (MSM98), Santa Clara, USA, April 6-8, 1998, 586-590.

[2] M. S. Mock, Solid-State Electron., 16, 1251, 1973.

[3] P.Norton, T.Braggins, and H.Levinstein, Phys. Rev. B, 8(12), 5632, 1973.

[4] K. Seeger, "Semiconductor Physics," 6th edn., Springer, 168-173, 1996.

[5] C. Erginsoy, Phys. Rev., 79, 1013, 1950.

[6] P. P. Debye and E. M. Conwell, Phys. Rev., 93(4), 693, 1954.

[7] S. S. Li and W. R. Thurber, Solid-State Electron., 20, 609, 1977.

[8] C. Herring and E. Vogt, Phys. Rev., 101(3), 944, 1956.

[9] Y. Kanda, IEEE Trans. Electron Devices, ED-29(1), 64, 1982.

[10] D. M. Caughey and R. E. Thomas, Proc. IEEE, 55, 2192, 1967.

[11] N. Arora, J. R. Hauser, and D. J. Roulston, IEEE Trans. Electron Devices, ED-29, 292, 1982.

[12] G. Masetti, M. Serveri, and S. Solmi, IEEE Trans. Electron Devices, ED-30, 764, 1983.

[13] G. Kaiblinger-Grüjin and S. Selberherr, Proc. Modeling and Simulation of Microsystems (MSM98), Santa Clara, USA, April 6-8, 1998, 70-75.

[14] W.Pietrenko, Phys. Status Solidi (A), 41(1), 197, 1977.

[15] K. Yamada, M. Nishihara, S. Shimada, M. Tanabe, M. Shimazoe, and Y. Matsuoka, IEEE Trans. Electron Devices, ED-29(1), 71, 1982.

[16] E. Ohta and M. Sakata, Jpn, J. Appl. Phys., 17(10), 1795, 1978.